



Title	Experimental MR imaging of zirconia ceramic joint implants at 1.5 and 3 T
Author(s)	Kamishima, T.; Kitamura, N.; Amemiya, M.; Ishizaka, K.; Kato, F.; Yasuda, K.; Shirato, H.; Terae, S.
Citation	Clinical Radiology, 65(5), 387-390 https://doi.org/10.1016/j.crad.2009.12.007
Issue Date	2010-05
Doc URL	http://hdl.handle.net/2115/43103
Type	article (author version)
File Information	CR65-5_387-390.pdf



[Instructions for use](#)

Title:

Experimental MR imaging of zirconia ceramic joint implants at 1.5T and 3 T

Introduction

Total joint arthroplasty is being increasingly performed in younger, more active patients, which necessitates improved implant longevity and enhanced component performance. Historically, cobalt-chromium has been the material of choice as a bearing surface for the femoral component in total knee arthroplasty (TKA). In recent years, ceramic components have been introduced as a bearing surface with superior resistance to surface roughening, improved frictional characteristics, and excellent biocompatibility as compared with cobalt-chrome. Despite the current success of TKA, postoperative complications such as peri-prosthetic fracture, infection, or loosening due to osteolysis remain. To increase the success rate in revision surgery, which includes determining potential bone graft needs, as well as implant inventory required to achieve a stable and durable reconstruction, accurate description of the proximity of intraosseous and soft tissue deposits to vital anatomical structure is important (1).

In the past decade, 3 tesla (3 T) magnetic resonance imaging (MRI) has developed and widespread as an excellent imaging method for evaluation of musculoskeletal diseases. However it is rarely used in evaluating orthopedic patients due to the susceptibility artifacts caused by implants. These metallic artifacts can be affected by type of material scanned (2, 3) and imaging parameters (4, 5). In our clinical

practice, we have found minimal artifact in the evaluation of alumina-ceramic implants compared with the traditional cobalt-chrome implants. Recently, zirconia, one of the newer ceramic, is introduced in the total joint surgery, which is tougher than alumina. Lee, et al. evaluated a new knee prosthesis with ceramic-surfaced oxidized zirconium (Zr-2.5Nb) femoral component using MR imaging and demonstrated 1.5 T MR images of oxidized zirconium implants using the fast spin echo sequence shows little image distortion (6). This information is encouraging for clinicians who investigate peri-prosthetic pathologies, however, the implant used in their study has a surface of zirconium oxide ceramic only approximately 5 μm in thickness. To our knowledge, decreased metal artifact with ceramic implant made of purely zirconia and improved image quality have not been described in the literature. In addition, there is no feasibility study on 3 T MR imaging of zirconia ceramic implants. It is true that zirconia ceramic are not ferromagnetic, but they do produce artifact in high field (3T) MR system (7). It is hardly predicted that no artifact generation is likely. Moreover, important factor in addition to the relative ferromagnetism is the shape of the components.

We hypothesized that 3 T MR images of zirconia ceramic implants have improved quality compared with 1.5 T MR images. Therefore, the purpose of this study

was to evaluate image quality and artifacts generated by cobalt-chrome and zirconia ceramic implants using 1.5 and 3 T MR scanners, and to ensure that MR imaging had no dangerous increase of temperature in and around the implants.

Materials and Methods

Two femoral implants for artificial knee joints of the same shape, one made of cobalt-chrome and the other of zirconia ceramic (LFA®-III, JMM, Osaka, Japan), were placed in 2 separate columnar acrylic phantoms (300 mm × 300 mm × 150 mm) filled with agar. Each implant was placed in the middle of the phantom (Figure 1).

After setting the direction of implants in the static magnetic field so that they are oriented in the same direction as in vivo scan, both were scanned with 1.5 T (Philips Intera scanner) and 3 T (Philips Intera Achieva scanner) MR system. Proton density weighted (PDW) images and short-inversion time inversion recovery (STIR) images were obtained, in axial, sagittal, and coronal planes (resulting in 6 scans for each session) for the zirconia ceramic implant, and in sagittal (resulting in 2 scans for each session) for the cobalt-chrom implant. The imaging parameters were modified from those proposed by Malchau H, et al. (8). The details of MR parameters are as shown in Table 1. Representative images are shown in Figure 2a-d. Images were graded by 2

radiologists according to the extent of the implant-derived artifacts: grade 1, negligible artifacts; there is almost no artifact that may influence the adjacent structures, grade 2, moderate artifacts; there are some artifacts, but the shape of the implant is recognizable, grade 3, remarkable artifacts; the shape of the implant is hardly recognized because of severe artifacts. To assess the extent of blooming effect two-dimensionally, thickness of zirconia ceramic implant was measured on MR images and compared with the actual thickness measured by a slide caliper (Plastic Digital Caliper PC-15JN, Mitsutoyo Co., Kawasaki, Japan). Measurement of thickness was done at the central portion (close to the bump at the site corresponding to the weight bearing area, shown in Figures) of the zirconia ceramic implants (Figure 2c and 2d). The thickness was measured 5 times at the same sites in 5 different acquisitions. To assess the extent of blooming effect three-dimensionally, volume of the implants were measured using MR data sets using commercially available workstation (ZIOSOFT, ZIOSOFT Inc., Tokyo, Japan). Representative image is shown in Figure 3. Volumery via water replacement method of implants was added 5 times and averaged for comparison. The regions of interest (ROI) sized 300-500 mm² were set in agar outside the zirconia ceramic (ROI-1, figure 2d) and air in the field of view (ROI-2). The signal was the mean value of the pixel intensity in the ROI-1 minus that of ROI-2. The noise was the standard deviation (SD) derived from

ROI-2. We measured signal-to-noise ratio (SNR) 5 times for each MR image. MR image analysis was performed using a workstation (Synapse, Fujifilm Medical, Tokyo, Japan). Temperature of the agar containing implants was measured before and after each session of MR scans using a non-contact infrared thermometer (Handy Thermo TVS200-EX, NEC, Tokyo, Japan). Figure 4 shows examples of thermographical image and measurement region of interest. Phantoms were kept in the MR scanning room until just before the temperature measurement. Temperature of the MR scanning rooms (1.5 T and 3T) and operation room where thermographical measurement was performed were 22 °C and 26 °C respectively.

Statistical Analysis

Mann-Whitney test was used for the assessment of the relationship between categorical data sets. Paired t-tests were used for the assessment of the relationship between quantitative data sets. A value of $p < 0.05$ was deemed as significant. Inter-observer agreement was estimated using calculations of the kappa value (κ). The kappa value ranges from -1 to +1. Kappa values are interpreted as follows: < 0.40 , poor to fair agreement; 0.41 to 0.60, moderate agreement; 0.61 to 0.80, substantial; 0.81 to 1.00, almost perfect agreement(9). MedCalc 7.4.4.0 statistical software package was

used for the statistical analysis.

Results

All the grading concerning the extent of the implant-derived artifacts for cobalt-chrome and zirconia ceramic implant was 3 and 1 respectively both for 1.5T and 3T system. The average rank of grading for implants-derived artifacts was larger for cobalt-chrome (n=4) than zirconia ceramic (n=12) implants (p=0.0036). Kappa value for the 2 observers was almost perfect ($\kappa=0.852$). The imaging artifacts generated by cobalt-chrome implant were remarkable at both 1.5T and 3T MR imaging, especially in 3T MR imaging (Figure 2a, b), making it impossible to measure the thickness of implant. On the other hand, zirconia ceramic implant had negligibly small artifacts at both 1.5 T and 3 T (Figure 2c, d). Averages of thickness measurement of zirconia ceramic implant were 8.1 mm, 8.7 mm, 8.2 mm, 8.4 mm, and 8.8 mm for 1.5 T STIR, 1.5 T PDW, 3 T STIR, 3 T PDW sagittal images, and by caliper respectively. Average values of repeated measurement of SNR were 133, 27, 414, and 110 for 1.5 T STIR, 1.5 T PDW, 3 T STIR and 3 T PDW images, respectively. The volume of zirconia ceramic implant by water replacement method was 25.0 ml. Difference in volume of zirconia ceramic implant between 1.5 T and 3 T systems were not statistically significant (paired

t-test, $p=0.39$) with a mean \pm SD of 28.7 ml \pm 3.6 ml ($n=5$) versus 29.5 ml \pm 3.4 ml ($n=6$) respectively. For one imaging data set (coronal STIR of 1.5 T), semiautomatic volumetry was not possible with ZIO software for unknown reason.

Thermographic measurement results before and immediately after MR imaging are shown in Table 2.

Discussion

The material of TKA components significantly affects the quality of MR images obtained. To the best of our knowledge, there have been no reports which evaluated the advantage of 3 T MR imaging over 1.5 T MR imaging in scanning implants of artificial joints, although Matsuura, et al. demonstrated that there were few artifacts with ceramic instrumentation even on 3T MR imaging in neurosurgical biomaterials (7). In this experimental study, zirconia ceramic implants produced minimal metal artifacts both in 1.5 T and 3 T MR imaging. Image quality as assessed by SNR was better with 3 T MR images, for both PDW and STIR sequences. Moreover, the thickness of implants measured on images of 1.5 T and 3 T MR images was almost the same as real thickness. There was no dangerous heating effect during MR imaging experiment. These results may suggest that we can safely obtain benefit from the higher SNR images of zirconia

ceramic implants using high strength MR systems. This study is limited by the fact that we have not tested if other component of artificial knee joint such as plastic and metal parts of tibial component may generate artifacts and heating effect. However, we believe that most artifacts from tibial component can be avoided by modifying the scan, such as swapping phase and frequency encoding direction, tilting view angle, increasing the read-out bandwidth, and decreasing voxel size. Also, previous investigations associated with 3 T MR imaging of various types of metallic implants have not shown any harmful heating (10). In summary, femoral implants of artificial knee joints made of zirconia ceramic can be safely scanned with better quality on 3 T MR imaging than 1.5 T MR imaging. In vivo studies of patients with total joint replacement are needed to obtain more conclusive information.

Acknowledgments

The authors thank Khin Khin Tha, MD, PhD for English language assistance, and for Riichiro Abe, MD, PhD for generous permission to use the non-contact infrared thermometer.

References

1. Weiland DE, Walde TA, Leung SB, Sychterz CJ, Ho S, Engh CA et al. Magnetic resonance imaging in the evaluation of periprosthetic acetabular osteolysis: A cadaveric study. *J Orthop Res* 2005;23:713-719
2. Wang Y, Truong TN, Yen C, Bilecen D, Watts R, Trost DW et al. Quantitative evaluation of susceptibility and shielding effects of nitinol, platinum, cobalt-alloy, and stainless steel stents. *Magn Reson Med* 2003;49:972-976
3. Nitatori T, Hanaoka H, Hachiya J, Yokoyama K. Mri artifacts of metallic stents derived from imaging sequencing and the ferromagnetic nature of materials. *Radiat Med* 1999;17:329-334
4. Viano AM, Gronemeyer SA, Haliloglu M, Hoffer FA. Improved mr imaging for patients with metallic implants. *Magn Reson Imaging* 2000;18:287-295
5. Olsen RV, Munk PL, Lee MJ, Janzen DL, MacKay AL, Xiang QS et al. Metal artifact reduction sequence: Early clinical applications. *Radiographics* 2000;20:699-712
6. Lee KY, Slavinsky JP, Ries MD, Blumenkrantz G, Majumdar S. Magnetic resonance imaging of in vivo kinematics after total knee arthroplasty. *J Magn Reson Imaging* 2005;21:172-178

7. Matsuura H, Inoue T, Ogasawara K, Sasaki M, Konno H, Kuzu Y et al. Quantitative analysis of magnetic resonance imaging susceptibility artifacts caused by neurosurgical biomaterials: Comparison of 0.5, 1.5, and 3.0 tesla magnetic fields. *Neurol Med Chir (Tokyo)* 2005;45:395-398; discussion 398-399
8. Malchau H, Potter HG. How are wear-related problems diagnosed and what forms of surveillance are necessary? *J Am Acad Orthop Surg* 2008;16 Suppl 1:S14-19
9. Landis JR, Koch GG. The measurement of observer agreement for categorical data. *Biometrics* 1977;33:159-174
10. Dietrich O, Reiser MF, Schoenberg SO. Artifacts in 3-t mri: Physical background and reduction strategies. *Eur J Radiol* 2008;65:29-35

Figure Legends

Figure 1 Photograph of an oxidized zirconium implant.

Table 1 Details of MR parameters used in this study.

PDW, proton density weighted; STIR, short-tau inversion recovery, ETL, echo train lengths; RBW, receiver bandwidth

Figure 2 Proton density-weighted MR images of a cobalt-chrome implant taken with 1.5 T (2a) and 3 T (2b) systems demonstrate remarkable artifacts and the shape of the implant is hard to recognize. The shapes of the implants were inserted as dotted lines.

Proton density-weighted MR images of an oxidized zirconium implant taken with 1.5 T (2c) and 3 T (2d) show minimal artifacts. Bumps corresponding to the weight bearing area are visualized. Thickness was measured at the portion close to the bumps (2c, arrows). The regions of interest (ROI) set in agar outside the zirconia ceramic is shown in figure 2d.

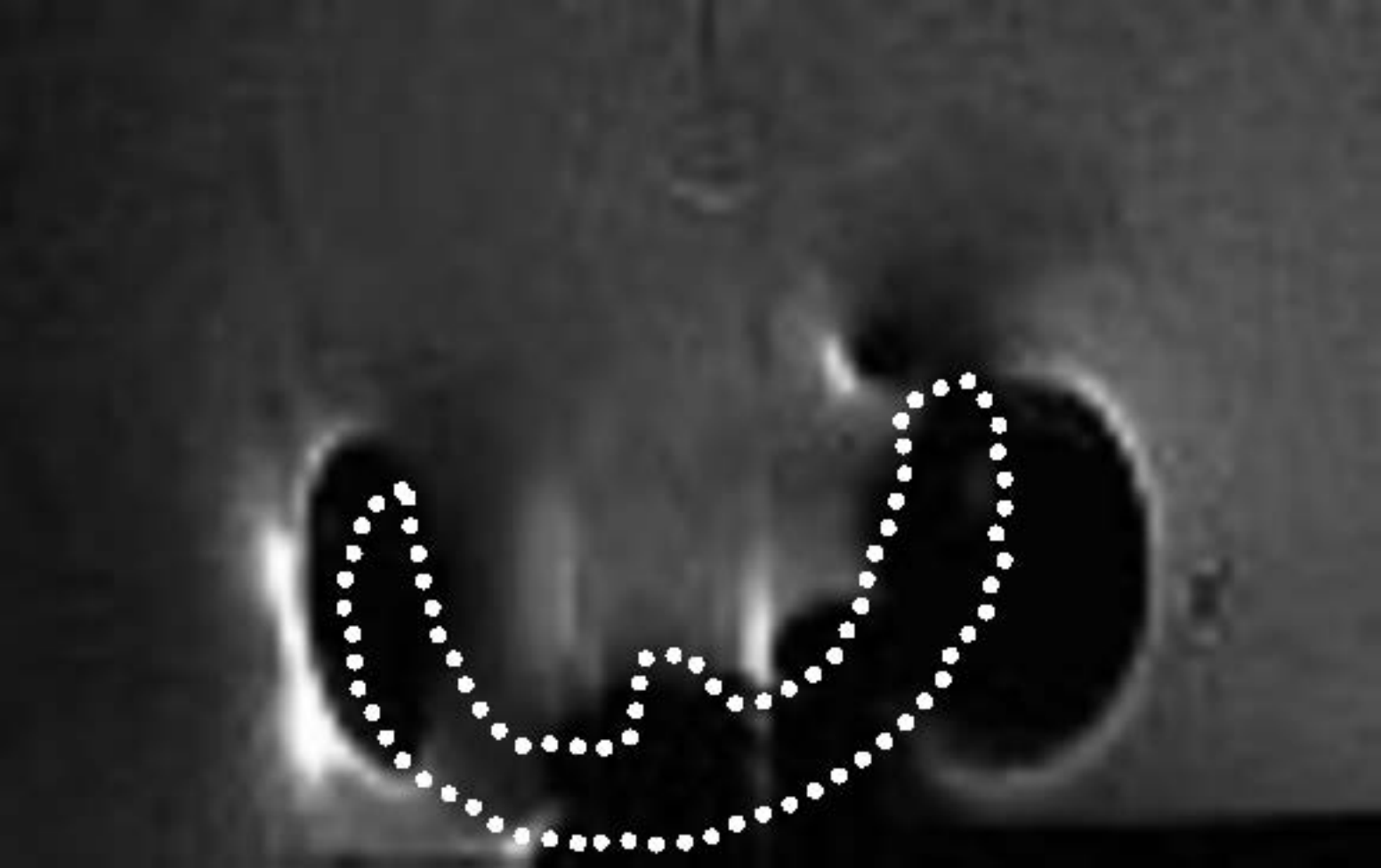
Figure 3 Reconstructed 3D image of zirconia ceramic implant using sagittal STIR image dataset obtained at 3 T system can be used for volumetry.

Figure 4 Thermography taken before and immediately after scanning oxidized zirconium implant with 3-T MR system. Change of color from yellowish to greenish indicates that the temperature decreases after the scan. Circular areas for figures of

pre-scanning (4a) and post-scanning (4b) represent the thermographical image taken from above.

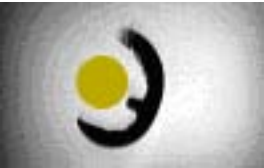
Table 2 Temperature of the agar containing zirconia ceramic measured before and after each session of MR scans

















Parameters	PDWI		STIR	
	1.5 T	3 T	1.5 T	3 T
TR (msec)	5000	5000	6000	6,000
TE (msec, effective)	30	30	17	17
TI (msec)	NA	NA	170	200
ETL	20	20	7	7
RBW (kHz/px)	312.5	312.5	438	438
FOV (cm)	18 x 18	18 x 18	20 x 20	20 x 20
Matrix	512 x 380	512 x 380	256 x 189	256 x 189
Slice thickness (mm)	3	3	4	4

Implant	1.5T		3T	
	Cobalt-chrome	Zirconia ceramic	Cobalt-chrome	Zirconia ceramic
Pre (°C)	21.2	23.2	21.9	22.0
Post (°C)	22.6	22.2	20.6	21.5